AUT Journal of Electrical Engineering

AUT J. Elec. Eng., 55(3) (Special Issue) (2023) 377-392
DOI: 10.22060/eej.2023.22092.5514

Fast $\mathcal{L}$asso-$\mathcal{MPC}$ Using Extended Kalman Filter for Robot-Assisted Rehabilitation: with Optimal Impedance

H. Ahmadian, H. A. Talebi*, I. Sharifi

Department of Electrical Engineering, Amirkabir University of Technology, Tehran, Iran

ABSTRACT: Elderly people may lose the ability to walk normally as their muscles weaken, or it may be difficult for them to maintain balance while walking. In addition to aging, nerve damage such as stroke, trauma, infectious diseases, accidents, ... may cause loss of balance in walking and weakening of muscles. Wearable robots are crucial for helping patients with lower limb diseases, particularly those with trouble walking since their numbers are rising. These robots assist patients in walking, provide comfort, and aid in recuperation. In this study, the fast model predictive control based on the $\mathcal{L}$asso regression theory ($\mathcal{L}$asso- $\mathcal{FMPC}$) and the extended Kalman filter ($\mathcal{EKF}$) was used to make a novel controller that helps the patient walk by adjusting the impedance so that, in addition to regular walking, the patient has to put out the most effort when walking. To evaluate the effectiveness of the proposed method, first, using OpenSIM software, the required torque data was determined for healthy, disabled, and sick people. Then, using these obtained data, the model fitting parameters were determined. In the end, experiments including a healthy person and a modular lower limb exoskeleton were performed. The findings show that the proposed method successfully estimates the patient's torque and correctly adjusts the robot's assistance level to the user's behavior, thereby maximizing his activity during treatment.

Review History:

Received: Jan. 21, 2023
Revised: Aug. 01, 2023
Accepted: Aug. 23, 2023
Available Online: Dec. 01, 2023

Keywords:

Extended Kalman Filter ($\mathcal{EKF}$)
$\mathcal{L}$asso Regression
Fast Model Predictive Control ($\mathcal{FMPC}$)
$\mathcal{L}$asso - $\mathcal{FMPC}$
Robot-Assisted Rehabilitation

1- Introduction

As the number of older people in the world grows at rates that have never been seen before, neuromuscular diseases related to getting older are becoming more common worldwide [1]. Now, more people want rehabilitation services than those who can get them, and the trend suggests that this difference may get more prominent in the future [2,3]. Assistive robotic devices could be one way to close the gap between the demand for and the supply of rehabilitation services [4]. Several robotic rehabilitation tools are presently available, and many more are under development. The most popular commercial robotic rehabilitation technologies for upper limb rehabilitation are sling-suspension-type [5], exoskeletons [6], and end-effector devices [7]. On the other hand, robotic exoskeletons treat specific joints while preventing dangerous or unhelpful compensatory movements that can happen when recovering with end-effector devices. Robotic physiotherapy has two operating modes: passive and active, depending on the degree of the patient's movement impairment [8]. Also, this treatment helps the patient's paralyzed arm avoid muscle atrophy, keep or improve its range of motion, get stronger, have less tone, and improve its ability to change [9,10].

Researchers have developed and deployed control techniques to address the control issues in rehabilitation. Most of the time, they deal with conventional methods like position and force control, two extreme examples of impedance control, computed torque control [11], sliding mode control [12, 13], $\mathcal{MPC}$ [14], robust adaptive control [15], fuzzy control [16], and neural network [18]. In addition, force control only works in confined places. The robot may need to initially be brought into touch with the environment using position control mode if it does not establish first contact with it. The force control mode can then be 27 turned on following that. However, moving between control modes is likely to cause inconsistent behavior. When the appropriate time to change the control mode is different from the appropriate time for a real environmental change, these unstable reactions may result. Impedance control (IC), which is excellent for dynamic systems with uncertain or time-varying properties, was utilized to make systems more compliant and safer to use when people were engaged, as was adaptive control $(\mathcal{AC})$, which was used for upper-limb rehabilitation robotic devices [19,20]. These two authors combined $\mathcal{IC}$ and $\mathcal{AC}$ methodologies to create adaptive impedance control $(\mathcal{AIC})$ systems. However, the $\mathcal{AC}$ method was based on inverse dynamics, which required acceleration measurement and reversibility of the anticipated inertia matrix. Measuring acceleration could be preferable because signals can be somewhat noisy. Implementing these control strategies is difficult since the computed inertia matrix's reversibility is

*Corresponding author's email: alit@aut.ac.ir

only sometimes attained.

The construction and management of a knee exoskeleton powered by a specialized rotating series elastic actuator $(\mathcal{SEA})$ were covered in [24]. To ensure safe contact with the patient, impedance control is used to enable the orthosis to change impedance during the gait phases. The development of $\mathcal{AIC}$ methods for robot-assisted rehabilitation can benefit from this property. An $\mathcal{AIC}$-based need-assistance system for ankle rehabilitation is proposed in [26]. The torque and kinematics data of the robot are used to assess the dynamic contribution of the patient during movement. The stiffness parameter of the impedance controller is next proposed to be calculated using two robot auxiliary control algorithms (complementary and optimum). This paper's evaluation of the suggested need-assistance solutions was expanded and published in [27, 28, 29]. So, a controller should be developed to offer the aid or changes required to accomplish educational tasks of rehabilitation by the patient's functional capacity. Corrective or assistance controllers are those that include these features.

Impedance control is frequently used to help patients during robot-assisted rehabilitation training activities, according to robot-assisted training with the feature of need-assistance [30]. Clinical investigations on stroke patients revealed that impedance control-based rehabilitation robots are more effective than robot-assisted therapy that only mimics conventional therapy at lowering upper limb muscular strength and enhancing patients' motor function [31, 32]. The patient's spatial flexibility is constrained despite the impedance control approach, allowing the patient's arm to stray from the training route. When patients veer from the intended course, assistance from the robot is constantly offered as a restorative force to assist them. Therefore, to maximize patient freedom, researchers have created an impedance-based demand-assistance technique that may be broadly split into two categories: strip-type controllers and window-type controllers. The patient's arm is free to roam around thanks to the window-type controller's predefined route and the moveable window. When the patient's arm is positioned outside the moving window, the robot's auxiliary force corrects the patient's arm toward the moving window [33, 34]. Another sort of band-type controller is based on a fault-tolerant region $(\mathcal{FTR})$, which establishes the inner and outer limits of $\mathcal{FTR}$ to produce a fault-tolerant band that permits patient movement. The window-type assist controller restricts the patient's spatial flexibility, whereas the strip-type assist controller grants the patient entire freedom and lets him pick his course without the robot's help. The patient's arm is completely free to move when it is in $\mathcal{FTR}$, but when it deviates from $\mathcal{FTR}$, the robot applies an auxiliary force to assist the patient's arm in completing the rehabilitation training job. Additionally, research has been done to find ways to give patients more independence. To expand the patient's spatial flexibility, in [35] first created a rope-based exoskeleton rehabilitation robot and then included a fault-tolerant zone surrounding the planned trajectory. The possibility of adding a plane channel around the predefined path based on a two-link rehabilitation robot was validated in [36]. The tape-type assistive controller has shown effective results in clinical studies, but it has a tendency - or "slackness"- that causes the patient to rely excessively on the helpful force [37]. The robot will not offer aid or correction as long as the patient's arm is within $\mathcal{FTR}$, significantly reducing the patient's active engagement. The $\mathcal{FTR}$ may be given a velocity curve to add, which causes a simulated movement in the $\mathcal{FTR}$. The controller produces a moving wall to force the patient's arm to move with the virtual motion to complete the training job and prevent laxity when the patient's arm is immobile or moving too slowly in $\mathcal{FTR}$.

The patient's effort during the rehabilitation process forms the foundation of the proposed $\mathcal{AC}$ systems. The torques and forces generated by the patient, as well as the stiffness and damping values of the patient's joints, can be used to quantify effort. It becomes apparent that it is necessary to evaluate the patient's torque and stiffness/damping characteristics when he interacts with active orthoses and exoskeletons. Torque given from the orthosis or other information sources, such as force sensors like a multi-axial load cell, can be used to estimate patient torque either directly or indirectly. This second approach has the major benefit of not utilizing force sensors, which lowers the overall cost of the device. [38] presents two methods for calculating interaction forces in robotic effectors. The first one combines a recursive estimating approach built on the least squares method with filtered dynamic equations. A generalized moment-based disturbance observer is part of the latter. Both techniques do away with the necessity to invert the inertial matrix and measure acceleration. The major objective of the best robot-assisted rehabilitation systems is to reduce the cost function associated with the rehabilitation aim and the patient-robot interaction [39]. According to [40], the interaction between a patient and a robot during a rehabilitation process is comparable to the interaction between a student and a teacher during a lesson. In this instance, the instructor (the robot) makes just a small attempt to reduce the student's (the patient's) mistake. The patient should exert the majority of the effort.

Even though $\mathcal{MPC}$ offers several benefits over traditional controllers, with this control, the desired performance may be stated as a single cost function that any user can quickly modify. Additionally, the reduction of the cost function in $\mathcal{MPC}$ control formulation guarantees both the tracking error and the smoothness of orthosis behavior. The wearer's comfort may be significantly and favorably impacted by this smoothness. The tracking error also demonstrates the controller's capacity to maintain a desired trajectory while accounting for external disturbances and uncertainties. Due to its conceptual simplicity and capability to handle complicated systems with numerous inputs, outputs, and rigid control requirements with ease, $\mathcal{MPC}$ has gained widespread acceptance in academia and industry [41-43]. Real-time $\mathcal{MPC}$ frameworks have been suggested in recent years [44-46] as a result of the work of researchers, and they have been used as control strategies in robotic applications, such as lower-limb, humanoids [47], mobile robots [48], and exoskeleton robots [49]. Additionally, robust tube-based $\mathcal{MPC}$ techniques have been created and presented for use with additional applications to deal with model uncertainties and outside disturbances [50]. By using this method, a control problem is transformed into a quadratic programming problem that may be resolved using several techniques, including gradient-based optimization [51], and neural networks [52]. The $\mathcal{MPC}$, which is regarded as a successful approach for resolving the latency issue, has been researched for need-assistance rehabilitation in the past. Using a delta robot and nonlinear $\mathcal{MPC}$, in [53] are optimized trainee skill level, motor learning, and training task completion for an upper body rehabilitation virtual task. Although this method shows promise for neuro-rehabilitation, it does not directly take into account joint behavior in humans. To control a simulated upper limb rehabilitation robot in the presence of disturbances, researchers investigated the use of $\mathcal{MPC}$. Task accuracy increased, but the method failed to separate human effort from external disruption [54]. By taking into account an upper-limb exoskeleton model and employing muscle activity for human joint torque estimation, in [55] utilized $\mathcal{MPC}$ for a 1-DOF upper limb rehabilitation task.

According to the literature review, the following open challenges still exist in the control of rehabilitation robots:

1) Most of the upper limb remote rehabilitation methods published in the literature are related to end-effector robots, which cannot ensure consistent and safe performance in each joint from the point of view of control systems.

2) In the literature, the interaction of the robot with the environment is not considered, or this interaction is considered with a constant force.

3) Failure to investigate the best enhancement of the therapist's skills with the robot.

4) Not predicting the torque created by the patient and not considering its effect on the robot torque.

5) The discussion of allocation of control has not been considered in any of the previous references.

Therefore, the contribution and the advantages of the proposed approach are summarized below:

1) The proposed approach satisfies the property of control allocation. That is, in this method, optimization is done in such a way that if the control force does not have much effect in one direction, it can be zero.

2) The proposed approach has faster calculations than other forecasting methods.

3) In the proposed approach, the $\mathcal{EKF}$ is used to estimate the torque of the patient, and with this estimated torque, the torque of the robot is optimized.

4) The main advantage of this work compared to other works is the use of OpenSim software to generate movement data for healthy and patient people and use it in simulation.

5) Accurate and fast performance of this method compared to other traditional $\mathcal{MPC}$ methods.

However, using robotic exoskeletons allows therapy to be conducted at the joint level because the human arm is coupled to the robot at various points. Most upper limb remote rehabilitation procedures published in the literature are for end-effector robots. In this paper, we employ torque feedback on several linkages to execute a targeted joint treatment and ensure compliant and secure performance at each joint from the standpoint of control systems. Safety and the capacity to react to human torque inputs with smooth and natural motion are of utmost importance when working with humans in the loop. The patient's torque is taken from OpenSim, an open-source software program for biomechanical modeling, simulation, and analysis, to improve the implementation of these algorithms. This study's primary contribution is to propose a fast model predictive control based on $\mathcal{L}$asso regression ($\mathcal{L}$asso-$\mathcal{FMPC}$) using the extended Kalman filter $\mathcal{EKF}$. The proposed controller assists the patient in walking by adjusting the impedance. In addition to regular walking, the patient has to exert the most effort while walking, and the system receives reasonable control allocation. The simulation results show the incredible effectiveness of the proposed control in robot-assisted rehabilitation.

This study's six sections are about a new control technique for robot-assisted rehabilitation. Following the introduction, the second section covers the system dynamic model of the rehabilitation robot. The third section discusses the Patient's torque observer with the $\mathcal{EKF}$. The controller and suggested $\mathcal{L}$asso-$\mathcal{FMPC}$ architecture is addressed in Section IV. Section V examines the simulation data to determine how effectively the suggested technique functions. The work's summation and expression are the focus of the final section.

2- System Dynamic Model

As just the swing phase is taken into account in this study, a 3-DOF planar vertical exoskeleton is assumed, and the model is shown as follows [21]:

$$M(q)\ddot{q}+C(q,\dot{q})\dot{q}+G(q)=\tau_a+\tau_{pat} \tag{1}$$

where $q\in\mathbb{R}^3$ is the joint angular position vector, $\dot{q}\in\mathbb{R}^3$ is the joint angular velocity vector, $\ddot{q}\in\mathbb{R}^3$ is the joint angular acceleration vector, $M(q)\in\mathbb{R}^{3\times3}$ is the inertia matrix calculated from the geometry of the manipulator, $C(q,\dot{q})\in\mathbb{R}^{3\times3}$ is the matrix containing the Coriolis effect and Centrifugal torques, $G(q)\in\mathbb{R}^3$ is the vector of gravity term, $\tau_a\in\mathbb{R}^3$ is the exoskeleton torque vector, τ_{pat} is the patient torque vector.

Due to control and designing the observer, the model state-space is expressed as (2).

$$\begin{aligned}
\dot{x}_q &= \underbrace{\begin{bmatrix} 0 & I & 0 \\ 0 & -M^{-1}C & -M^{-1}G \\ 0 & 0 & 0 \end{bmatrix}}_{A_q} x_q + \underbrace{\begin{bmatrix} 0 \\ M^{-1} \\ 0 \end{bmatrix}}_{B_q} (\tau_a+\tau_{pat}) \\
x_q &= \begin{bmatrix} \theta \\ \dot{\theta} \\ 1 \end{bmatrix}
\end{aligned} \tag{2}$$

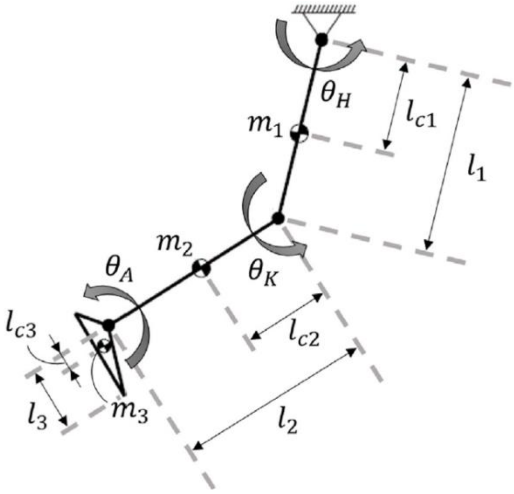

(a)

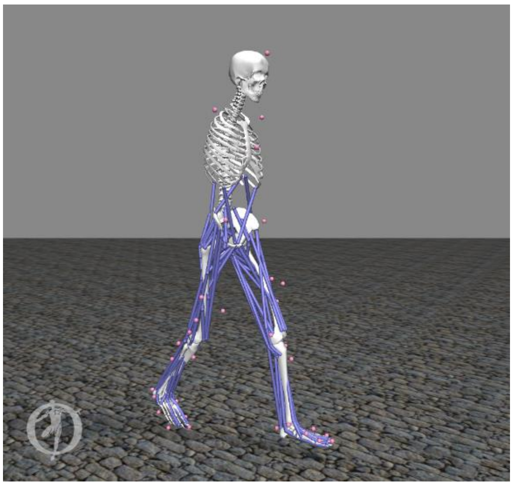

(b)

Fig. 1. (a) During the swing phase, a schematic illustration of the user-exoskeleton model is shown. , and are the center of mass locations, length, joint angle, and mass of the i-th link, respectively [22], (b) A view of the schematic in OpenSim.

where, A_q and B_q are the state matrix and input matrix, respectively.

Fig. 1 depicts a schematic illustration of the patient-exoskeleton model. The ankle and hip joints are denoted by the subscripts A and H, respectively.

According to Figure 1. a, the following assumptions are also considered in this study:

1- The center of mass of each link is assumed to be exactly in the middle of the link.

2- The mass of links is completely different.

3- The moment of inertia of the third link (ankle) is assumed to be very small.

3- Patient's Torque Observer with $\mathcal{EKF}$

The $\mathcal{EKF}$ used for estimating the patient's torque is discussed in this section. The generalized momenta, abbreviated p, is the definition of the filtered variable. This study's nonlinear model is provided by:

$$\begin{aligned} \dot{p} &= f(p) + w \\ z &= h(p) + v \end{aligned} \tag{3}$$

here

$$f(p) = \tau_a + C^T(q,\dot{q})\dot{q} - G(q)$$
$$h(p) = p = M(q)\dot{q} \tag{4}$$

where w and v are white Gaussian noise with a mean of 0, the selection of the process variance matrices and measurement noises was based on the tuning recommendations made in [22]. Each time the $\mathcal{EKF}$ is used, a time-varying gain L_k is generated. Therefore, the patient moments may be approximated as follows:

$$r(k) = L_k(p(k) - \hat{p}(k))$$
$$\hat{\tau}_{pat}(k) = L_k^{-1}\left(\frac{r(k) - r(k-1)}{\Delta t}\right) + r(k) \tag{5}$$

in which Δt is the sample time, $p(k) = H(q(k))\dot{q}(k)$, and $\hat{p}(k)$ is the expected generalized momenta. Using $\mathcal{EKF}$ for patient torque estimation, an examination of disturbance observer-based techniques was reported in [23].

4- $\mathcal{L}asso - \mathcal{FMPC}$ for Optimal Impedance

With the $\mathcal{MPC}$, the starting state is the system's state at each sampling moment, and the control action is decided by solving an optimal control problem based on a finite horizon model. Even though the optimization process makes a control sequence with a finite number of steps, the plant only gets the first control action [16,17]. [18] says that the best way to do rehabilitation is for the patient and the robot to work together as a teacher and a student.

A teacher (the robot) and a student (the patient) are two agents that work together to do the same thing. The goal of walking rehab is to reduce the error $\tilde{q} = q^d - q$ for a given expected trajectory q^d or to make the person walk in a way that looks like what is wanted. While the student (the patient) is being guided or told to follow the trajectory, the teacher (the robot) works as little as possible, limiting its torque (τ_a) and increasing the student's torque (τ_b).

4- 1- Model Predictor

The actuators torque, τ_a, is specified as follows to implement the $\mathcal{L}$asso $\mathcal{FMPC}$:

$$\tau_a = K_r\left(q^d - q\right) - B_r\dot{q} \tag{6}$$

where K_r and B_r are the robot controller's damping and stiffness settings. Since it is presumed that impedance-controlled series elastic actuators move exoskeleton joints, they are characterized in this way.

The development of the system over a finite horizon may be predicted by numerical integration using (6), the patient-exoskeleton dynamics model, (1), the patient torques calculated in the preceding section, and the joint beginning locations and velocities (specified as the present ones). The fourth-order Runge-Kutta algorithm is applied in this article.

4- 2- Objective Function

Applied torque, τ_a, and the tracking error, $\tilde{q} = q^d - q$, should be included in the objective function to be minimized. Therefore, this case is also considered in the following definition.

Definition 1. : $\mathcal{L}$asso $-\mathcal{FMPC}$

The model predictive control problem based on the $\mathcal{L}$asso regression theory is expressed as follows:

$$V_N^o(\tilde{q}) = \min_{\underline{\tau_a}}\left\{V_N(\tilde{q},\underline{\tau_a}) \triangleq F(\tilde{q}_N) + \sum_{j=0}^{N-1}\ell\left(\tilde{q}_j,\tau_{aj}\right)\right\}$$
$$s.t.:$$
$$\tau_{aj} \in \mathbb{U},\quad \tilde{q}_j \in \mathbb{X},\quad j = 0,\ldots,N-1 \tag{7}$$

with

$$\ell\left(\tilde{q}_j,\tau_{aj}\right) = \tilde{q}_j^T Q\tilde{q}_j + \tau_{aj}^T R\tau_{aj} + \left\|S\tau_{aj}\right\|_1, \tag{8}$$

with $\underline{\tau_a}^T = \left[\tau_{a_0}^T \ \cdots \ \tau_{a_{N-1}}^T\right]$, and S is a constant matrix. Q and R are positive definite weighted matrices. The $\mathcal{L}$asso $-\mathcal{FMPC}$ executes the first action of the optimum policy, $\tau_a(k) = \tau_{a_0}^\star$, at the current state, $\tilde{q} = \tilde{q}(k)$, at each iteration k. This action is determined by the online solution of (7), (8). The obtained implicit control law is also considered as $K_N(\tilde{q}) \equiv \tau_{a_0}^\star$ [24].

The main purpose of using $\mathcal{L}$asso regression theory in $\mathcal{MPC}$ is to take advantage of the main features of this regression, such as control allocation, feature selection, filtering, and application to systems with fast dynamics and machine learning. This makes the lasso method very useful and efficient, especially for systems that are too active and need to allocate control and adjust simultaneously. The characteristics of this regression and other regressions and their comparison are fully explained in [25].

4- 3- Optimization Problem

The gradient descent optimization approach has been used in this study to minimize the cost function $J(K_r(k))$. Given that the cost function's (triangle down $J(K_r(k))$) negative gradient tends to move in the direction of its lowest values, the approach is based on iterative optimization.

$K_r(k-1)$, the previous optimal value, is the initial value of K_r for the optimization process. Since instant k contains only one optimization update, the value of $K_r(k)$ is given by:

$$K_r(k) = K_r(k-1) - \eta\nabla J\left(K_r(k)\right) \tag{9}$$

where η is the step size of the optimization.

Table 1. Model fitting parameters

a_{hip0}	-6.9	a_{hip1}	-10.85
b_{hip2}	27	ω_{hip}	$5.14\,{rad}/{sec}$
a_{knee_0}	-9.42	a_{knee_1}	-3.79
b_{knee_2}	-26.1	ω_{knee}	$10.09\,{rad}/{sec}$
a_{ankle}	-35.18	a_{ankle_1}	58.1
b_{ankle_2}	12.98	ω_{ankle}	$5.08\,{rad}/{sec}$

Table 2. Model dynamic parameter

m_1	$7.2\,Kg$	L_1	$0.4410\,m$
m_2	$3.3480\,Kg$	L_2	$0.4428\,m$
m_3	$10.0440\,Kg$	L_3	$0.0702\,m$
J_1	$0.4668\,Kg.m^2$	L_{1CoM}	$0.2205\,m$
J_2	$0.2188\,Kg.m^2$	L_{2CoM}	$0.2214\,m$
J_3	$0.0017\,Kg.m^2$	L_{3CoM}	$0.0351\,m$

5- Simulation Results

As previously stated, since the human arm is connected to the robot at numerous locations, adopting robotic exoskeletons enables therapy to be carried out at the joint level. The majority of published material on upper limb remote rehabilitation techniques uses end-effector robots. To conduct a targeted joint treatment and guarantee compliant and secure performance at each joint from the perspective of control systems, we use torque feedback on multiple linkages in this research. When dealing with humans in the loop, safety and the ability to respond to human torque inputs with fluid and natural motion are of the utmost significance. To enhance the execution of these algorithms, the patient's torque is collected from OpenSim, an open-source tool for biomechanical modeling, simulation, and analysis. To determine patient torques in OpenSim software, it is necessary to select a function with a known oscillation frequency. The oscillation frequency of this model, which is believed to be its most significant characteristic, is used to replicate the patient torque using a sinusoidal function. As a result, OpenSim software was used to acquire torque data for a typical, healthy human stride, and by fitting the $f(t)=a_0+a_1\cos(\omega t)+b_1\sin(\omega t)$ function to the data in Fig. 2, the values in Table 1 were obtained.

To validate the controller introduced in the previous sections, in this section, we will simulate the dynamic model with the $\mathcal{L}asso\_\mathcal{FMPC}$ controller introduced for impedance control. For simulation, all sections are discrete at 200 Hz, and the parameters in Table 2 are used to simulate the system. The following values are used for system noise Γ_1 and measurement noise Γ_2 for the observer.

$$\begin{aligned}\Gamma_1 &= \mathrm{diag}([0.001,0.001,0.001,0.001,0.001,0.001])\\ \Gamma_2 &= \mathrm{diag}([0.05,0.05,0.05,0.05,0.05,0.05,\\ &\quad 0.03,0.03,0.03,0.01,0.01,0.01])\end{aligned} \tag{10}$$

and objective function parameters selected as follows:

$$\begin{aligned}Q &= 1500^{*}\,\mathrm{diag}([8,4,3])\\ R &= 0.001^{*}\,\mathrm{diag}([0.2,0.7,1])\end{aligned} \tag{11}$$

In order to check the performance of the proposed controller, the data of a healthy human walking path was needed. for this purpose, using the program OpenSim, we generated the required trajectory of healthy human standard gait data. Then we used these data to test the proposed controller to determine the movement of the patient by the robot. The simulation results for the output of the path traversed by the patient with the help of the robot are shown in Figure 3. As can be seen, the proposed method performs well in following the desired state.

The $\mathcal{EKF}$ observer, seen in Figure 4 of the earlier torque estimate findings, was utilized to get the patient torque estimation employed in the $\mathcal{LFMPC}$ controller. The oscillation frequency measured at each joint in the preceding

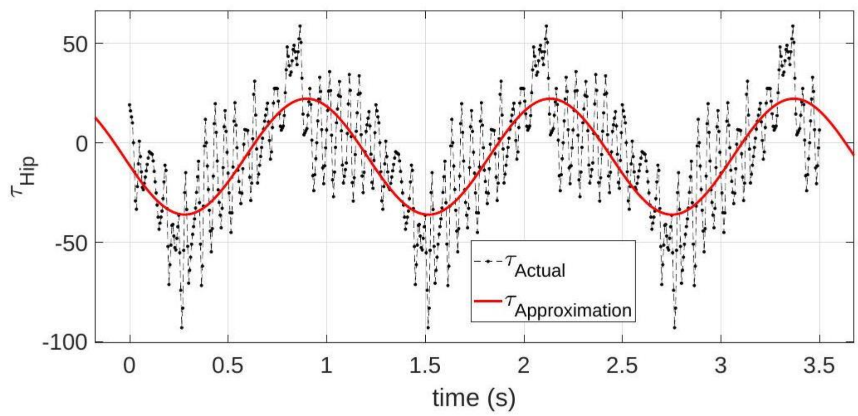

(a) Hip torque

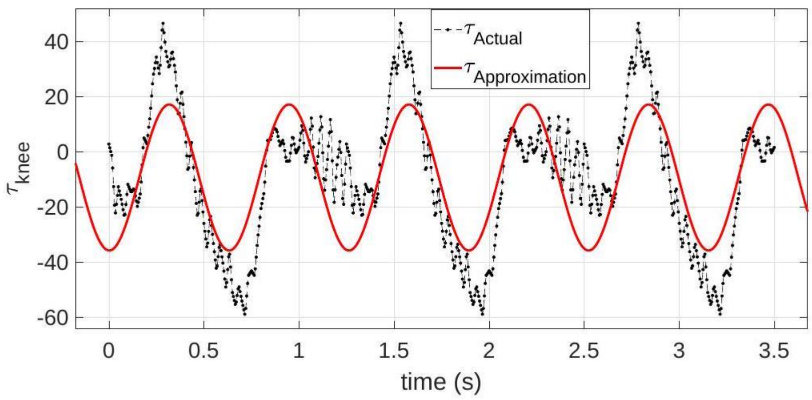

(b) Knee torque

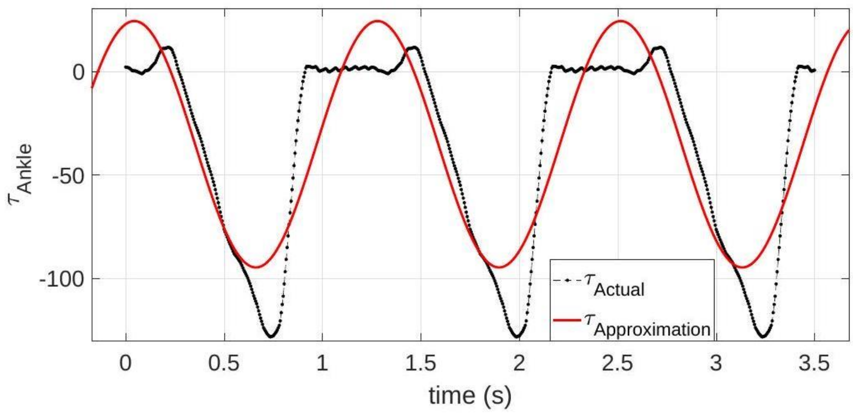

(c) Ankle torque

Fig. 2. The approximation of normal gait torques with $A_d sin(\omega_0 t)$.

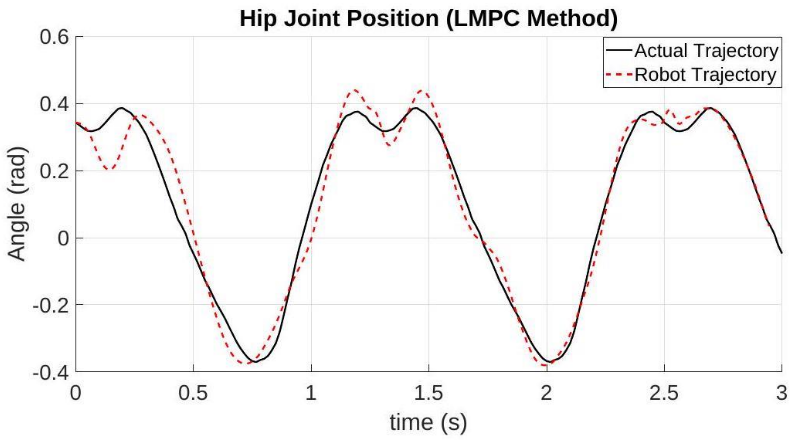

(a) Hip

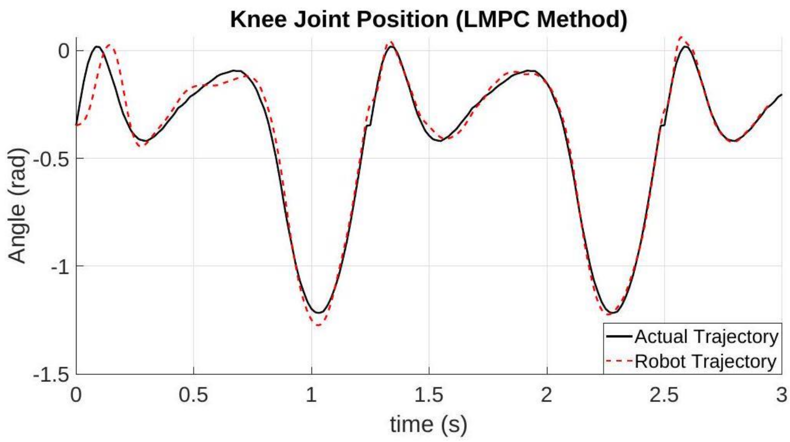

(b) Knee

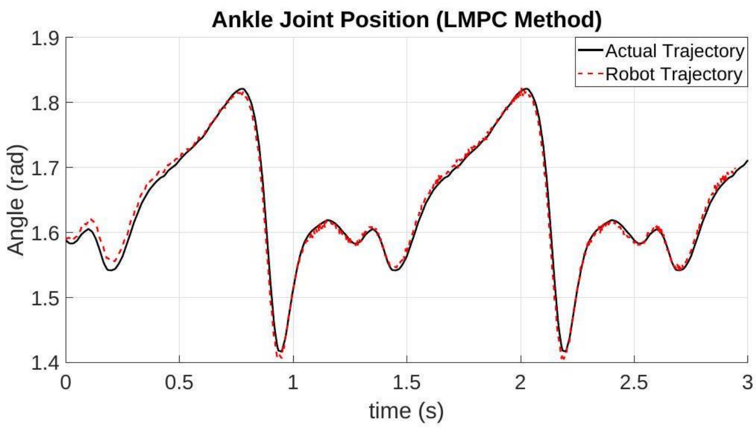

(c) Ankle

Fig. 3. The patient's trajectory with a robot versus with the standard gait (using $\mathcal{LFMPC}$ method).

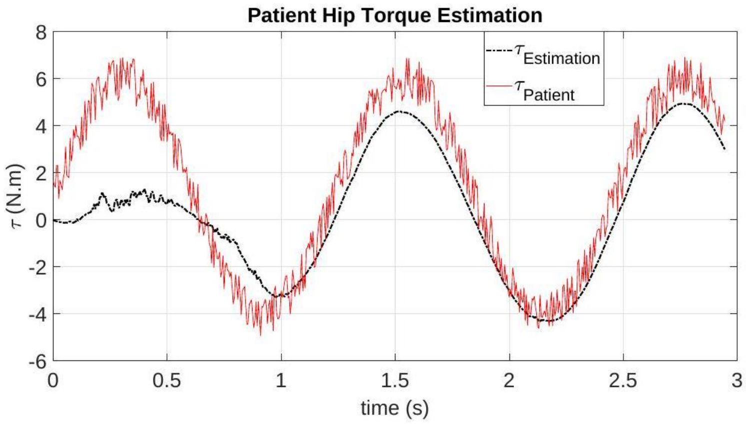

(a) Hip

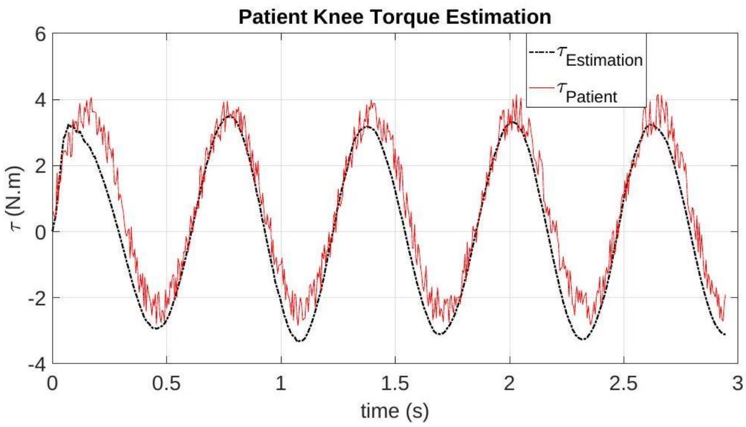

(b) Knee

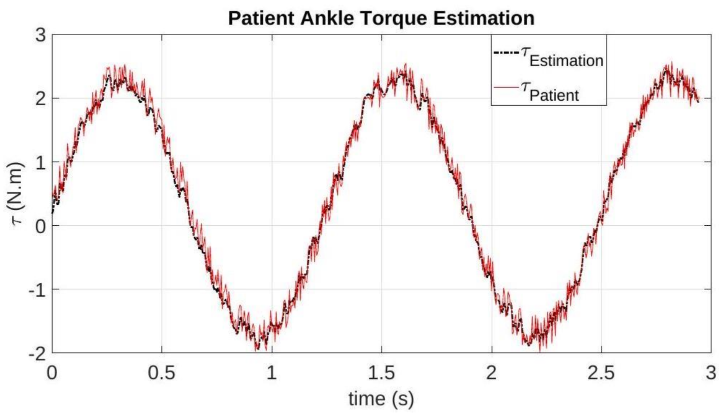

(c) Ankle

Fig. 4. The estimation of patient torque using $\mathcal{EKF}$.

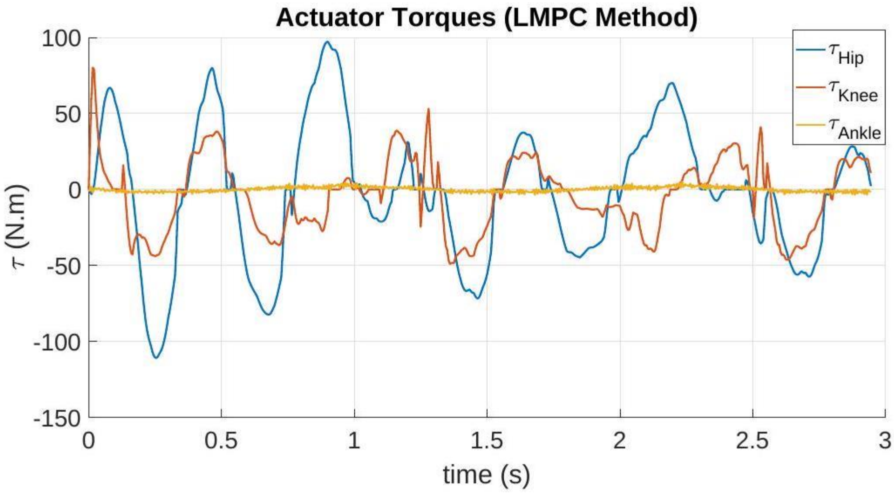

(a) The result for optimization with fmincon function of MATLAB.

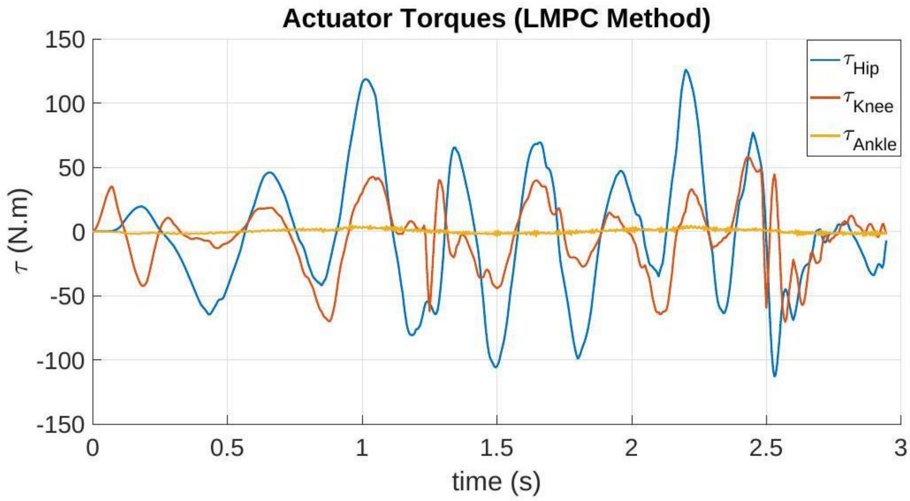

(b) The result for optimization with gradient method.

Fig. 5. The control effort signal for actuator torques (using $\mathcal{LFMM}$ method).

section is utilized to simulate.

The ideal control efforts have been optimized using two different techniques. The first is the gradient approach suggested in the controller section, and the second is the $\mathcal{LFMPC}$ controller optimization problem using the MATLAB fmincon function.

Figure 5 displays the outcomes of the actuators' produced torques (control signal). While using fmincon decreases torques, the quality of the intended trajectory is also diminished. The adoption of the gradient approach is justified by the fact that it is 20 times quicker and has a lower computing cost than other optimization techniques.

In order to evaluate and compare the performance of the proposed method, the classic $\mathcal{MPC}$ method was similarly used for simulation (this work was done in [22], with the difference that the motion data of the healthy person was not used and only a smooth trajectory was assumed to move). The simulation results are shown in Figure 6. As you can see, the robot could not move the patient in the trajectory of healthy human behavior, and the error is high. But in the

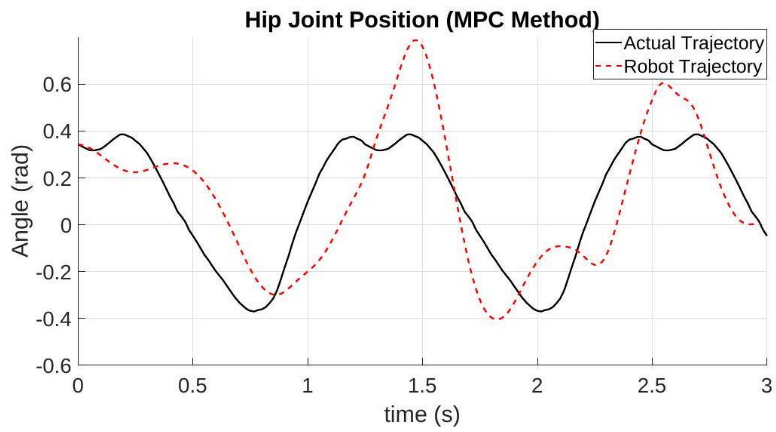

(a) Hip

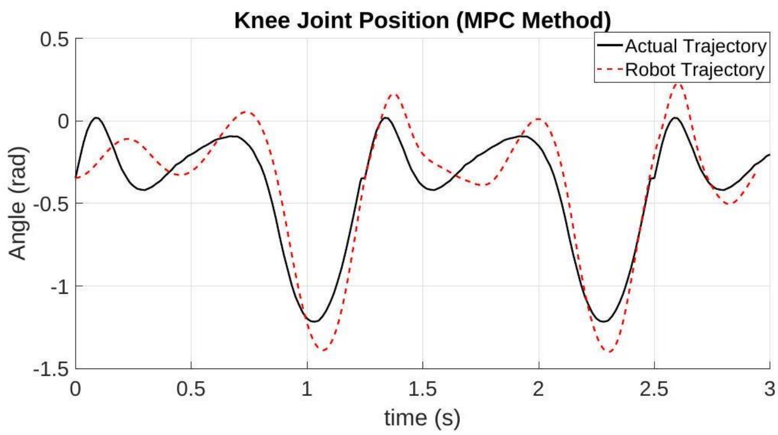

(b) Knee

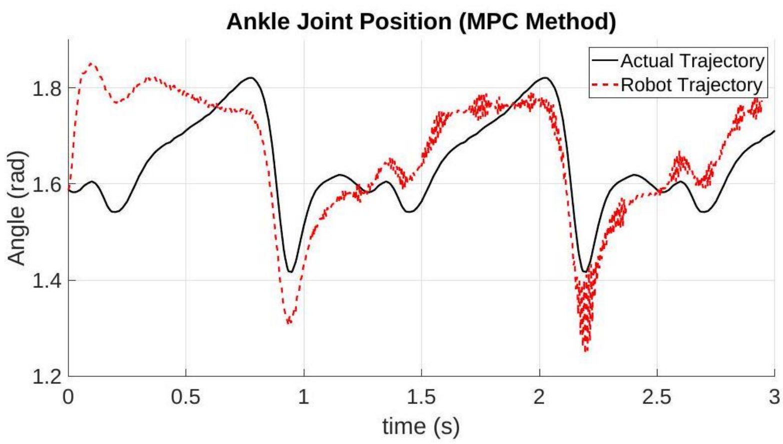

(c) Ankle

Fig. 6. The patient's trajectory with a robot versus with the standard gait (using $\mathcal{MPC}$ method).

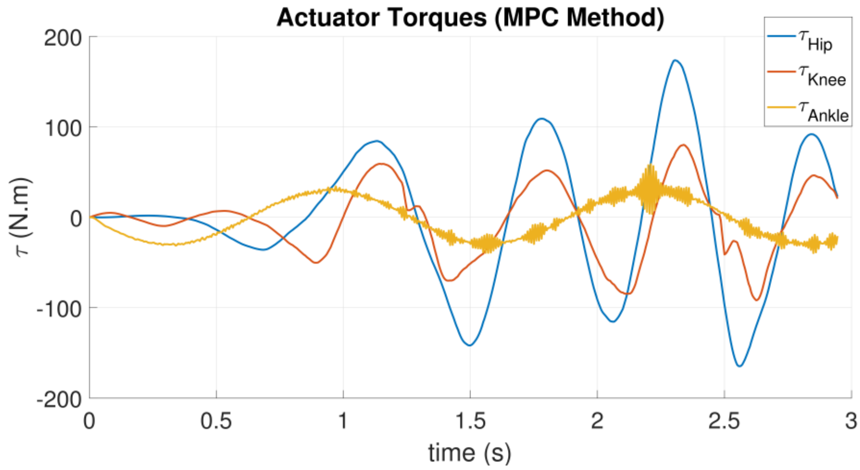

Fig. 7. The control effort signal for actuator torques (using $\mathcal{MPC}$ method).

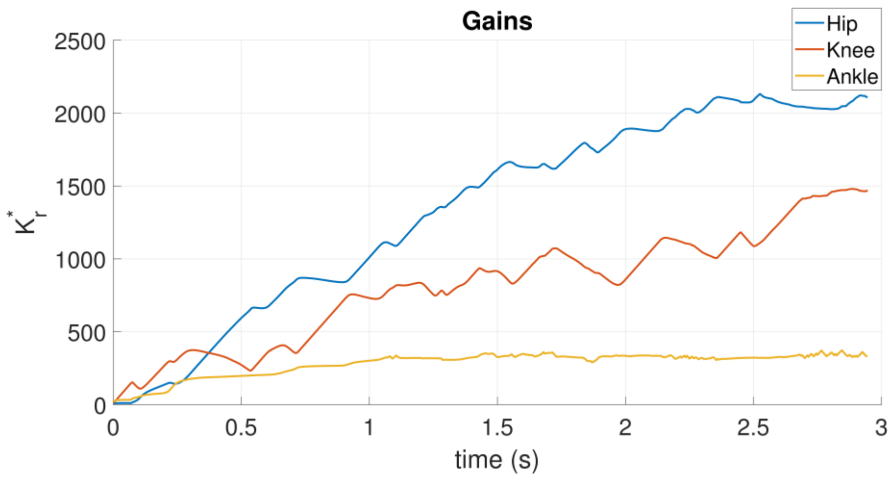

Fig. 8. update with gradient method.

proposed method (Figure 3), the robot has been able to follow the movement trajectory of a healthy human.

Also, to compare the two methods in terms of control efforts, the control efforts with the classical $\mathcal{MPC}$ method are also shown in Figure 7. By comparing this result with the control efforts of the proposed method (Figure 5), it can be seen that there is control allocation in the proposed method and a control force is always almost zero.

Figure 8 displays proportional gain values for each stage of the gradient approach as determined by the $\mathcal{L}asso\_\mathcal{FMPC}$ controller.

6- Conclusion

This study is a component of continuing work to create individualized and adaptable controllers for robot-assisted rehabilitation. In this study, an online $\mathcal{L}asso$ - $\mathcal{FMPC}$ method based on the assessment of patient torque is used to determine the ideal stiffness parameters for exoskeleton impedance control. The $\mathcal{EKF}$ method and the generalized momenta-based disturbance observer are used to calculate the patient's torque during the swing phase. To assess the effectiveness of the suggested control strategy, experiments were carried out involving a healthy subject and a modular lower limb exoskeleton. The findings demonstrate that the suggested method successfully estimates the patient's torque and correctly adjusts the level of robot assistance to the user's behavior, thereby maximizing his or her activity during therapy. Future research will involve a patient-based clinical study to determine whether the suggested approach can be a valuable tool for enhancing neuronal plasticity following stroke and thereby enhancing motor rehabilitation.

References

[1] F. Yuan, E. Klavon, Z. Liu, R.P. Lopez, X. Zhao, A systematic review of robotic rehabilitation for cognitive training, Frontiers in Robotics and AI, 8 (2021) 605715.

[2] T.-Y. Kim, S.-H. Kim, H. Ko, Design and implementation of BCI-based intelligent upper limb rehabilitation robot system, ACM Transactions on Internet Technology, 21(3) (2021) 1-17.

[3] H. Ahmadian, I. Sharifi, H.A. Talebi, Robust Distributed Lasso-Model Predictive Control Design: A Case Study on Large-Scale Multi-Robot Systems, AUT Journal of Modeling and Simulation, 55(1) (2023) 8-8.

[4] H. Ahmadian, H.A. Talebi, I. Sharifi, $\mathcal{L}$ 1– $\mathcal{BL}$ Adaptive Controller Design for Wrist Rehabilitation Robot, in: 2021 9th RSI International Conference on Robotics and Mechatronics (ICRoM), IEEE, 2021, pp. 177-184.

[5] G. Bauer, Y.-J. Pan, H. Shen, Adaptive impedance control in bilateral telerehabilitation with robotic exoskeletons, in: 2020 IEEE International Conference on Systems, Man, and Cybernetics (SMC), IEEE, 2020, pp. 719-725.

[6] M.A. Gull, S. Bai, T. Bak, A review on design of upper limb exoskeletons, Robotics, 9(1) (2020) 16.

[7] J. Durrer, P. Agrawal, A. Ozgul, S.C. Neuhauss, N. Nama, D. Ahmed, A robot-assisted acoustofluidic end effector, Nature Communications, 13(1) (2022) 6370.

[8] G. Gugliandolo, G. Campobello, P.P. Capra, S. Marino, A. Bramanti, G. Di Lorenzo, N. Donato, A movement-tremors recorder for patients of neurodegenerative diseases, IEEE Transactions on Instrumentation and Measurement, 68(5) (2019) 1451-1457.

[9] Q. Wu, X. Wang, B. Chen, H. Wu, Patient-active control of a powered exoskeleton targeting upper limb rehabilitation training, Frontiers in Neurology, 9 (2018) 817.

[10] H. Kalani, S.M. Tahamipour-Z, I. Kardan, A. Akbarzadeh, Assistive Control of a Hip Exoskeleton Robot, using a DQN-Adjusted Delayed Output Feedback Method, AUT Journal of Electrical Engineering, 55(1) (2023) 99-106.

[11] B. Brahmi, M. Driscoll, I.K. El Bojairami, M. Saad, A. Brahmi, Novel adaptive impedance control for exoskeleton robot for rehabilitation using a nonlinear time-delay disturbance observer, ISA transactions, 108 (2021) 381-392.

[12] Y. Zhang, G. Cao, W. Li, J. Chen, L. Li, D. Diao, A self-adaptive-coefficient-double-power sliding mode control method for lower limb rehabilitation exoskeleton robot, Applied Sciences, 11(21) (2021) 10329.

[13] N.A. Alawad, A.J. Humaidi, A.S. Alaraji, Observer sliding mode control design for lower exoskeleton system: Rehabilitation case, Journal of Robotics and Control (JRC), 3(4) (2022) 476-482.

[14] H. Ahmadian, H.A. Talebi, I. Sharifi, $\mathscr {L} _ {1} $ Adaptive Control Design Using CMPC: Applied to Single-Link Flexible Joint Manipulator, in: 2021 29th Iranian Conference on Electrical Engineering (ICEE), IEEE, 2021, pp. 709-714.

[15] J. Wang, O.R. Barry, Inverse optimal robust adaptive controller for upper limb rehabilitation exoskeletons with inertia and load uncertainties, IEEE Robotics and Automation Letters, 6(2) (2021) 2171-2178.

[16] R. Sharma, P. Gaur, S. Bhatt, D. Joshi, Optimal fuzzy logic-based control strategy for lower limb rehabilitation exoskeleton, Applied Soft Computing, 105 (2021) 107226.

[17] A. Sheybanifar, S.M. Barakati, Simplified Model Predictive for Controlling Circulating and Output Currents of a Modular Multilevel Converter, AUT Journal of Electrical Engineering, 54(1) (2022) 121-136.

[18] T. Lee, I. Kim, S.-H. Lee, Estimation of the continuous walking angle of knee and ankle (talocrural joint, subtalar joint) of a lower-limb exoskeleton robot using a neural network, Sensors, 21(8) (2021) 2807.

[19] H. Ahmadian, M. Lotfi, M.B. Menhaj, H.A. Talebi, I. Sharifi, A novel L1 adaptive-hybrid control with guaranteed stability for a class of uncertain nonlinear systems: A case study on SA330 Puma, Journal of the Franklin Institute, 359(17) (2022) 9860-9885.

[20] R. Nasiri, M. Shushtari, A. Arami, An adaptive assistance controller to optimize the exoskeleton contribution in rehabilitation, Robotics, 10(3) (2021) 95.

[21] H. Ahmadian, H.A. Talebi, I. Sharifi, $\mathcal{L}$1 Adaptive Control Design for SRS Robot Using Gaussian Process Regression, in: 2021 7th International Conference on Control, Instrumentation and Automation (ICCIA), IEEE, 2021, pp. 1-6.

[22] W.M. dos Santos, A.A. Siqueira, Optimal impedance via model predictive control for robot-aided rehabilitation, Control Engineering Practice, 93 (2019) 104177.

[23] J.C. Jaimes, A.A. Siqueira, Preliminary evaluation of disturbance torque estimation approaches for lower-limb robotic rehabilitation, in: 2019 IEEE 16th International Conference on Rehabilitation Robotics (ICORR), IEEE, 2019, pp. 715-720.

[24] M. Gallieri, M. Gallieri, Principles of LASSO MPC, Lasso-MPC–Predictive Control with ℓ1-Regularised Least Squares, (2016) 47-63.

[25] L. Etienne, K. Langueh, L. Rajaoarisoa, Self-triggered controller co-design using LASSO regression, in: 2022 30th Mediterranean Conference on Control and

Automation (MED), IEEE, 2022, pp. 139-144.

[26] F. De Gaitani, W. dos Santos, A.A.G. Siqueira, Design and performance analysis of a compact series elastic actuator for exoskeletons, Journal of Control, Automation and Electrical Systems, 33(3) (2022) 1012-1021.

[27] Y. Hu, J. Meng, G. Li, D. Zhao, G. Feng, G. Zuo, Y. Liu, J. Zhang, C. Shi, Fuzzy Adaptive Passive Control Strategy Design for Upper-Limb End-Effector Rehabilitation Robot, Sensors, 23(8) (2023) 4042.

[28] X. Ai, V. Santamaria, I. Omofuma, S.K. Agrawal, Effects of Boundary-Based Assist-As-Needed Force Field on Lower Limb Muscle Synergies during Standing Posture Training, IEEE Transactions on Neural Systems and Rehabilitation Engineering, (2023).

[29] J.M. Lopes, J. Figueiredo, C. Pinheiro, L.P. Reis, C.P. Santos, Biomechanical assessment of adapting trajectory and human-robot interaction stiffness in impedance-controlled ankle orthosis, Journal of Intelligent & Robotic Systems, 102(4) (2021) 76.

[30] P. Song, Y. Yu, X. Zhang, A tutorial survey and comparison of impedance control on robotic manipulation, Robotica, 37(5) (2019) 801-836.

[31] H.I. Krebs, J.J. Palazzolo, L. Dipietro, M. Ferraro, J. Krol, K. Rannekleiv, B.T. Volpe, N. Hogan, Rehabilitation robotics: Performance-based progressive robot-assisted therapy, Autonomous robots, 15 (2003) 7-20.

[32] H.I. Krebs, B.T. Volpe, D. Williams, J. Celestino, S.K. Charles, D. Lynch, N. Hogan, Robot-aided neurorehabilitation: a robot for wrist rehabilitation, IEEE transactions on neural systems and rehabilitation engineering, 15(3) (2007) 327-335.

[33] Q. Wu, B. Chen, H. Wu, Adaptive admittance control of an upper extremity rehabilitation robot with neural-network-based disturbance observer, IEEE Access, 7 (2019) 123807-123819.

[34] H.J. Asl, T. Narikiyo, M. Kawanishi, An assist-as-needed control scheme for robot-assisted rehabilitation, in: 2017 American control conference (ACC), IEEE, 2017, pp. 198-203.

[35] X. Cui, W. Chen, X. Jin, S.K. Agrawal, Design of a 7-DOF cable-driven arm exoskeleton (CAREX-7) and a controller for dexterous motion training or assistance, IEEE/ASME Transactions on Mechatronics, 22(1) (2016) 161-172.

[36] H.J. Asl, M. Yamashita, T. Narikiyo, M. Kawanishi, Field-based assist-as-needed control schemes for rehabilitation robots, IEEE/ASME Transactions on Mechatronics, 25(4) (2020) 2100-2111.

[37] M. Casadio, V. Sanguineti, Learning, retention, and slacking: a model of the dynamics of recovery in robot therapy, IEEE Transactions on Neural Systems and Rehabilitation Engineering, 20(3) (2012) 286-296.

[38] H. Kalani, S.M. Tahamipour-Z, I. Kardan, A. Akbarzadeh, Assistive Control of a Hip Exoskeleton Robot, using a DQN-Adjusted Delayed Output Feedback Method, AUT Journal of Electrical Engineering, 55(1) (2023) 99-106.

[39] N. Naghavi, A. Akbarzadeh, S.M. Tahamipour-Z, I. Kardan, Assist-As-Needed control of a hip exoskeleton based on a novel strength index, Robotics and Autonomous Systems, 134 (2020) 103667.

[40] N. Jarrassé, T. Charalambous, E. Burdet, A framework to describe, analyze and generate interactive motor behaviors, PloS one, 7(11) (2012) e49945.

[41] I. Jammeli, A. Chemori, H. Moon, S. Elloumi, S. Mohammed, An assistive explicit model predictive control framework for a knee rehabilitation exoskeleton, IEEE/ASME Transactions on Mechatronics, 27(5) (2021) 3636-3647.

[42] E. Nejabat, A. Nikoofard, Hybrid Robust Model Predictive Based Controller for a Class of Multi-Agent Aerial dynamic Systems, AUT Journal of Electrical Engineering, 54(2) (2022) 209-224.

[43] Y. Cao, J. Huang, Neural-network-based nonlinear model predictive tracking control of a pneumatic muscle actuator-driven exoskeleton, IEEE/CAA Journal of Automatica Sinica, 7(6) (2020) 1478-1488.

[44] A. Sheybanifar, S.M. Barakati, Simplified Model Predictive for Controlling Circulating and Output Currents of a Modular Multilevel Converter, AUT Journal of Electrical Engineering, 54(1) (2022) 121-136.

[45] A. Saleh, A. Deihimi, Model Predictive Control of Distributed Energy Resources with Predictive Set-Points for Grid-Connected Operation, AUT Journal of Electrical Engineering, 50(2) (2018) 109-120.

[46] S. Li, Y. Shi, L. Hu, Z. Sun, A generalized model predictive control method for series elastic actuator driven exoskeleton robots, Computers & Electrical Engineering, 94 (2021) 107328.

[47] S. Katayama, M. Murooka, Y. Tazaki, Model predictive control of legged and humanoid robots: models and algorithms, Advanced Robotics, 37(5) (2023) 298-315.

[48] Y. Hu, H. Su, L. Zhang, S. Miao, G. Chen, A. Knoll, Nonlinear model predictive control for mobile robot using varying-parameter convergent differential neural network, Robotics, 8(3) (2019) 64.

[49] N. Dunkelberger, S.A. Carlson, J. Berning, K.C. Stovicek, E.M. Schearer, M.K. O'Malley, Shared control of elbow movements with functional electrical stimulation and exoskeleton assistance, in: 2022 International Conference on Rehabilitation Robotics (ICORR), IEEE, 2022, pp. 1-6.

[50] A.J. Prado, M. Torres-Torriti, F.A. Cheein, Distributed tube-based nonlinear MPC for motion control of skid-steer robots with terra-mechanical constraints, IEEE Robotics and Automation Letters, 6(4) (2021) 8045-8052.

[51] R. Tallamraju, S. Rajappa, M.J. Black, K. Karlapalem,

A. Ahmad, Decentralized mpc based obstacle avoidance for multi-robot target tracking scenarios, in: 2018 IEEE International Symposium on Safety, Security, and Rescue Robotics (SSRR), IEEE, 2018, pp. 1-8.

[52] T. Salzmann, E. Kaufmann, J. Arrizabalaga, M. Pavone, D. Scaramuzza, M. Ryll, Real-time neural MPC: Deep learning model predictive control for quadrotors and agile robotic platforms, IEEE Robotics and Automation Letters, 8(4) (2023) 2397-2404.

[53] C.J. Ostafew, A.P. Schoellig, T.D. Barfoot, Robust constrained learning-based NMPC enabling reliable mobile robot path tracking, The International Journal of Robotics Research, 35(13) (2016) 1547-1563.

[54] N. Scianca, D. De Simone, L. Lanari, G. Oriolo, MPC for humanoid gait generation: Stability and feasibility, IEEE Transactions on Robotics, 36(4) (2020) 1171-1188.

[55] C. Caulcrick, W. Huo, E. Franco, S. Mohammed, W. Hoult, R. Vaidyanathan, Model predictive control for human-centred lower limb robotic assistance, IEEE Transactions on Medical Robotics and Bionics, 3(4) (2021) 980-991.

[56] M. Gallieri, Lasso-MPC–Predictive Control with l1-Regularised Least Squares, Springer, 2016.

HOW TO CITE THIS ARTICLE

H. Ahmadian, H. A. Talebi, I. Sharifi, Fast Lasso-MPC Using Extended Kalman Filter for Robot-Assisted Rehabilitation: with Optimal Impedance, AUT J. Elec. Eng., 55(3) (Special Issue) (2023) 377-392.

DOI: 10.22060/eej.2023.22092.5514

Archive of SID.ir